ChemComm

Accepted Manuscript

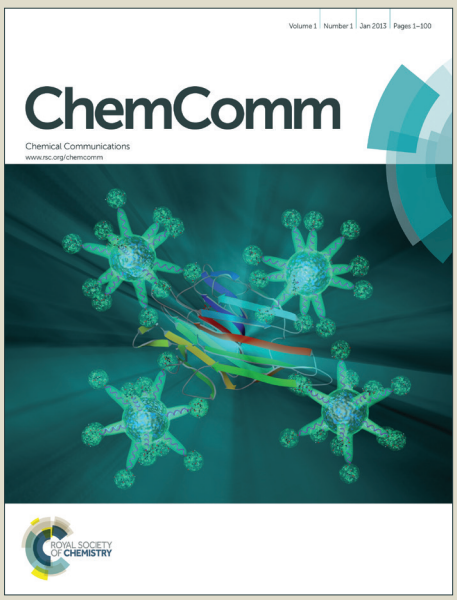

ROYAL SOCIETY OF CHEMISTRY

www.rsc.org/chemcomm

Cite this: DOI: 10.1039/c0xx00000x

www.rsc.org/xxxxxx

ARTICLE TYPE

Mechanical exfoliation of track-etched two-dimensional layered materials for ultrathin nanopores

Yanan Jiang,[a] Jun Gao,[c] Wei Guo,*[b] and Lei Jiang[ab]

Received (in XXX, XXX) XthXXXXXXXXX 20XX, Accepted Xth XXXXXXXXX 20XX

DOI: 10.1039/b000000x

Mechanical exfoliation of ion-track-etched two-dimensional layered materials yields nanometer-thin nanoporous sheets that can be suspended atop a silicon window to controllably fabricate single- or multi-pore nanofluidic devices.

Over the past one or two decades, synthetic nanopores in solid-state materials have gained considerable attention as a research platform for biochemical sensing, water treatment, energy harvesting, and etc.[1] Typically in such nanofluidic systems, the pore size can be well controlled down to 1 nm,[2] but the pore length is still restricted to the thickness of the substrate materials. Although the state-of-the-art micro- and nanofabrication techniques reduce the membrane thickness down to sub-100 nm,[3] particularly in several types of silicon-based materials, the spatial resolution of the nanopore sensor is still far from the requirement of single-molecular detection that individual translocation events in transmembrane ionic current is induced by merely one molecular target.[4]

Until recently, two-dimensional (2D) materials, including mono- or few-layer graphene,[5] boron nitride,[6] and molybdenum disulfide,[7] are used as the membrane substrate that further reduces the pore length down to the atomic scale. In these 2D materials-based nanofluidic devices, the 2D nanocrystals are firstly grown on a metal substrate through chemical vapor deposition method and afterwards transferred onto a windowed silicon chip.[5] The nanopore is then drilled in the 2D membrane with a focused electron beam in a transmission electron microscope. These atomically thin nanopore devices have been conceptually proved for DNA translocation and sequencing.[8] One fatal problem of this approach is the sophisticated material processing steps, and thus, the yield of such devices cannot be scale-up for real-world applications.

In fact, many natural layered materials, showing strong in-plane chemical bonds, but weak van der Waals-like interlayer coupling, such as graphite and some minerals, represent a diverse source of the ultrathin nanopore membranes for mass production and facile processing.[9] In this communication, taking muscovite mica for example, we demonstrate the produce of nanometer-thin nanoporous sheets by mechanical exfoliation of ion-track-etched 2D layered materials (Figs. 1A and 1B). These nanoporous mica thin sheets can then be transferred onto a silicon window to controllably fabricate single- or multi-pore nanofluidic devices (Fig. 1C).

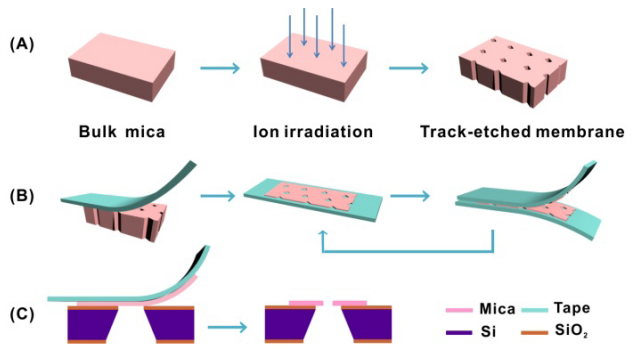

Fig.1 Mechanical exfoliation of track-etched mica sheet yielding ultrathin nanoporous membrane for nanofluidic device. (A) Bulk mica sheet is irradiated by swift heavy ion beam, and chemically etched with hydrofluoric acid to produce nanopores in the bulk membrane. (B) A sticky tape is firstly attached to the surface of the nanoporous bulk mica membrane, and is repeatedly peeled off with other pieces of fresh tape. (C) Peeled thin mica flakes can be transferred onto a solid silicon window yielding a suspended nanopore membrane.

Bulk muscovite mica is a representative type of two-dimensional layered materials, consisting of alternating aluminum (or magnesium) stabilized silicate tetrahedra.[10] The thickness of individual mica monolayer is ca. 1 nm. To drill nanopores in the bulk mica membrane, it was firstly irradiated by swift heavy ions with ion flux density of 10^8 or 10^5 per cm^2. The initial thickness of the bulk mica membrane is about 10μm. After chemically etched by hydrofluoric acid (HF) solution, the latent ion tracks were developed into diamond-shaped, high-aspect-ratio nanopores (Fig. S1, ESI).[11] Scanning electron microscopic (SEM) observations show that the length of the major axis (l_{maj}) of the diamond-shaped nanopores increases linearly with the etching time, from several tens to hundreds of nanometers.[12] Mechanical exfoliation of the chemically etched mica membrane using a scotch tape-based method yields nanometer-thin nanoporous mica flakes laying on the solid substrate (Fig. S2, ESI). These peeled mica nanoflakes become visible due to the difference in interference color,[13] when they are placed onto a silicon substrate with a 400-nm-thick, oxidized capping layer (Fig. S3, ESI). This feature facilitates further identification and manipulation of the tiny flakes for practical use. The thickness of the mica nanoflakes can be stepwisely reduced via the repeated peel-off from the parent bulk materials. Then the ultrathin mica sheets can be optically selected depending on the interference color. The

nanopore size is determined by the chemical etching process, and is independent of the mechanical exfoliation. Therefore, in this study, we etched the latent ion tracks into wide nanopores (l_{maj}~100-400 nm), so that the whole mica thin flakes and the nanopores therein could be clearly shown in an identical vision.

Further precise characterization of the lateral size and thickness of the mica nanoflakes were carried out with an atomic force microscope (AFM). Typical images were shown in Fig. 2A and Fig. S4, and the results were summarized in Fig. 2B. The membrane thickness can be remarkably reduced down to about 10-nm via the mechanical exfoliation, while retaining the lateral size of sub-micron to tens of microns. The membrane thickness shows a rough positive correlation with respect to the lateral size of the mica flakes. A large portion of the membrane thickness concentrates in the range of 20-300 nm. The lateral size of single- or few-layer (n<10) mica flakes ranges from several hundred nanometers to several microns that makes it difficult to handle for further use (Fig. S4).

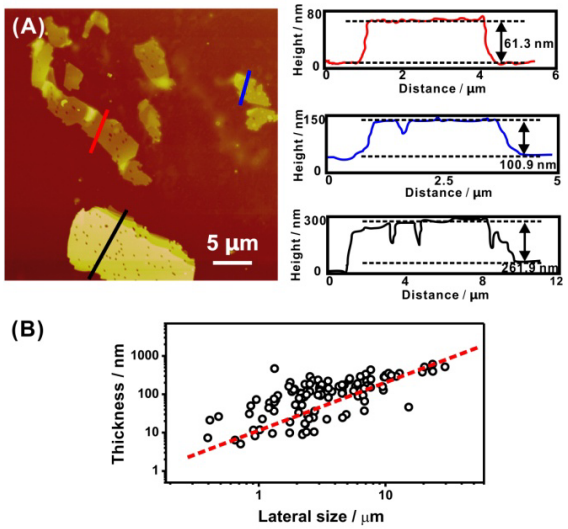

Fig. 2 AFM characterization of the nanoporous mica thin membranes. (A) Typical AFM image of the mica thin flakes, and the corresponding height profiles. The thickness is ranging from several tens to several hundred nanometers. (B) The membrane thickness increases with their lateral size. Data points were collected from over one hundred measured nanoflakes. The ion track density is ~10^8/cm^2.

Using similar methods, the peeled mica nanoflakes can be transferred onto a silicon window yielding a suspended ultrathin nanopore membrane. The silicon window was embedded in a 400-μm-thick Si/SiO_2 bilayer structure, with a large opening of 560 μm and a small opening of about 10 μm (Fig. 1C). The experimental setup was confirmed by both optical microscope (Fig. 3A) and SEM (Fig. 3B). Individual mica nanoflakes can be eventually found to fully cap the silicon window on the small end. For the case shown in Fig. 3C, there are about 60 nanopores located in the testing area of 10 μm× 10 μm, and the mean l_{maj} is about 166 nm.

By placing electrolyte solution and electrodes on the two sides of the suspended nanoporous mica membrane (Fig.S5, ESI), we further study the ion transport properties through the mica nanochannels at various electrolyte concentrations. As shown in Fig. 3D, at high potassium chloride (KCl) concentration range (0.01-1 M), the transmembrane ionic conductance through the mica nanochannels increases linearly with the KCl concentration. But at low KCl concentrations below 10^{-3} M, the ionic conductance shows saturation with respect to the electrolyte concentration. Since the mica surface takes excess negative charge,[14] this conductance saturation at low electrolyte concentrations indicates a surface-governed ion transport behavior.[15] By taking the Debye-Hückel approximation,[16] the Debye screening length is about 96.3 nm at ~10^{-5} M. This result is in line with the pore size measured by SEM observation (insert in Fig. 3C). Parallel ionic conducting tests were performed on separate suspended mica membranes with different l_{maj}. A rough linear relationship is found between the total ionic conductance and the pore area, suggesting the availability of the nanopore devices (Fig. S6, ESI).

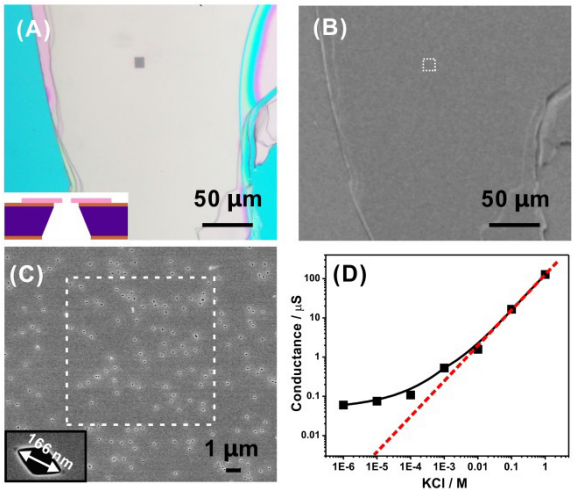

Fig. 3 Nanoporous mica membrane is suspended atop a silicon window opened in a 400-μm-thick Si/SiO_2 substrate. Both optical (A) and SEM images (B) show that the silicon window was fully covered by the mica flakes. The dashed frames in (B) and (C) indicate the underneath silicon window. (C) Magnified view of the nanoporous mica membrane. The insert shows the diamond-shaped naopore, etched by 5M HF solution for 60 minutes. The length of the major axis (l_{maj}) is about 166 nm. The membrane thickness is ca. 700 nm. (D) Transmembrane ionic conductance measured in KCl electrolyte with various concentrations. Surface-governed ion transport is found at low concentration below 10^{-3} M. The dashed line represents the bulk conductivity.

By reducing the ion track density down to 10^5/cm^2, the exact pore number in the testing area can be precisely controlled, yielding single-pore nanofluidic devices. Statistical results of fifty separate samples show three representative types of the suspended ultrathin mica membrane containing non-, one-, or two-nanopore within the area of the underneath silicon window (side length ~10 μm, Figs. 4A-4C). Since the mean track density is very low, nearly 80% of the exfoliated membranes do not include any track-etched nanopores within the testing area (Fig. 4D). About 20% of the tested samples contain precisely single-nanopore. And less than 2% of the exfoliated membranes contain two or more pores. The mean ion track density of 10^5/cm^2 indicates a mean pore number of 0.1 pores in an area of 100 μm^2. But the local pore density can be deviate from the average value.[17] Thus, large portion of the exfoliated membranes contain no pores. It is reasonable to expect a ca. 20% yield of single-pore device. This value is still noteworthy for modern nanotechnolgy and nanofabrication techniques.

We also test the ion conducting properties of the single- and double-nanopore devices. Linear *I-V* responses are found for the exfoliated mica nanopores (Fig. 4E and Fig. S7), suggesting the nanopores are geometrically symmetric. Moreover, we confirm that there is no measurable leak current through the suspended mica membrane, if there are no nanopores in it (Fig. 4E and Fig. S8). The exfoliated mica membrane provides a perfect seal onto the silicon window through van der Waals interactions with the substrate. Restricted to the relatively large side length of the underneath silicon window, the thickness of the suspended mica membrane can be as large as several hundred nanometers (refer to Fig. 2B). To further reduce the size of the silicon windows, for example down to sub-micron scale, atomically thin nanoporous sheets can be used to cap the windows. Besides mica, this nanopore fabrication technique can be generally applied to other dielectric layered materials, including some layered metal oxides and silicates.[18]

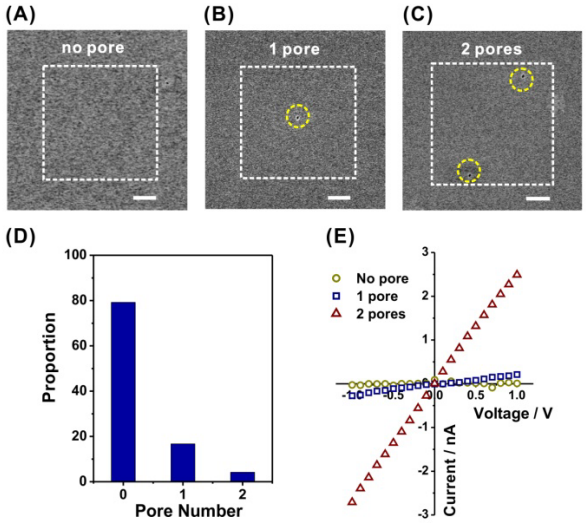

Fig. 4 Mechanical exfoliation of low-density tracked mica membrane yields single-pore nanofluidic devices. (A-C) Representative examples containing zero, one, or two nanopores within the testing area. The track density here is ~10^5/cm^2. The dashed frames indicate the underneath silicon window (10 μm × 10 μm) and the dashed circles indicate the individual nanopores. The scale bar is 2 μm. (D) Statistical results show the probability of the exfoliated mica nanosheets with fixed pore number. (E) *I-V* responses of the single- and double-nanopore devices in 0.1 M KCl solution. No leak current can be measured if there is no nanopore in the mica membrane. The membrane thickness is about 1-3 microns.

In conclusion, we demonstrate an effective and easy-to-use approach to produce nanometer-thin nanoporous sheets by mechanical exfoliation of ion-track-etched mica membrane. The nanoporous ultrathin mica sheets can be further developed into single- or multi-pore nanofluidic devices by simply suspending them onto a silicon window. The size, length, and number of the nanopores can be well controlled by using this method. This approach can be generally applied to other two-dimensional layered materials to fabricate atomically thin membranes with predesigned patterns or structures for ultrafiltration, water purification, and desalination.

This work is financially supported by the National Research Fund for Fundamental Key Projects (2011CB935700, 2013CB934104), the National Natural Science Foundation of China (21103201, 11290163, 91127025, 21121001). The Chinese Academy of Sciences is gratefully acknowledged under the Key Research Program of the CAS (KJZD-EW-M01).

Notes and references

[a] *Key Laboratory of Bio-Inspired Smart Interfacial Science andTechnology of Ministry of Education, School of Chemistry and Environment, Beihang University, Beijing 100191, P. R. China.*
[b] *Laboratory of Bio-inspired Smart Interface Science, Technical Institute of Physics and Chemistry, Chinese Academy of Sciences, Beijing 100190, P. R. China.*
E-mail: wguo@iccas.ac.cn.
[c] *Beijing National Laboratory for Molecular Sciences (BNLMS), Key Laboratory of Organic Solids, Institute of Chemistry, Chinese Academy of Sciences, Beijing 100190, P.R. China.*
† Electronic Supplementary Information (ESI) available: materials and processing steps of track-etched mica membrane, experimental setup of the nanofluidic device, ionic conductance measurements with respect to the pore area, and the test of leak current. See DOI: 10.1039/b000000x/

1 (a) W. Guo, Y. Tian and L. Jiang, *Acc. Chem. Res.*, 2013, **46**, 2834; (b) S. Majd, E. C. Yusko, Y. N. Billeh, M. X. Macrae, J. Yang and M. Mayer, *Curr. Opin. Biotechnol.*, 2010, **21**, 439; (c) W. Sparreboom, A. van den Berg and J. C. T. Eijkel, *Nat. Nanotechnol.*, 2009, **4**, 713. (d) J. Gao, W. Guo, D. Feng, H. Wang, D. Zhao, and L. Jiang, *J. Am. Chem. Soc.*, 2014, **136**, 12265.
2 C. Dekker, *Nat. Nanotechnol.*, 2007, **2**, 209.
3 (a) I. Vlassiouk, P. Y. Apel, S. N. Dmitriev, K. Healy and Z. S. Siwy, *Proc. Natl. Acad. Sci. U. S. A.*, 2009**, 106**, 21039; (b) B. N. Miles, A. P. Ivanov, K. A. Wilson, F. Dogan, D. Japrung and J. B. Edel*, Chem. Soc. Rev.*, 2013**, 42**, 15.
4 (a) D. Branton, D. W. Deamer, A. Marziali, H. Bayley, S. A. Benner, T. Butler, M. Di Ventra, S. Garaj, A. Hibbs, X. Huang, S. B. Jovanovich, P. S. Krstic, S. Lindsay, X. S. Ling, C. H. Mastrangelo, A. Meller, J. S. Oliver, Y. V. Pershin, J. M. Ramsey, R. Riehn, G. V. Soni, V. Tabard-Cossa, M. Wanunu, M. Wiggin and J. A. Schloss, *Nat. Biotechnol.*, 2008, **26**, 1146; (b) B. M. Venkatesan and R. Bashir, *Nat. Nanotechnol.*, 2011, **6**, 615.
5 S. Garaj, W. Hubbard, A. Reina, J. Kong, D. Branton and J. A. Golovchenko, *Nature*, 2010, **467**, 190.
6 S. Liu, B. Lu, Q. Zhao, J. Li, T. Gao, Y. Chen, Y. Zhang, Z. Liu, Z. Fan, F. Yang, L. You and D. Yu, *Adv. Mater.*, 2013, **25**, 4549.
7 K. Liu, J. Feng, A. Kis and A. Radenovic, *ACS Nano*, 2014, **8**, 2504.
8 C. A. Merchant, K. Healy, M. Wanunu, V. Ray, N. Peterman, J. Bartel, M. D. Fischbein, K. Venta, Z. Luo, A. T. C. Johnson and M. Drndić, *Nano Lett.*, 2010, **10**, 2915.
9 (a) K. S. Novoselov, D. Jiang, F. Schedin, T. J. Booth, V. V. Khotkevich, S. V. Morozov and A. K. Geim, *Proc. Natl. Acad. Sci. U. S. A.*, 2005, **102**, 10451; (b) A. Castellanos-Gomez, M. Wojtaszek, N. Tombros, N. Agrait, B. J. van Wees and G. Rubio-Bollinger, *Small*, 2011, **7**, 2491; (c) J. N. Coleman, M. Lotya, A. O'Neill, S. D. Bergin, P. J. King, U. Khan, K. Young, A. Gaucher, S. De, R. J. Smith, I. V. Shvets, S. K. Arora, G. Stanton, H. Y. Kim, K. Lee, G. T. Kim, G. S. Duesberg, T. Hallam, J. J. Boland, J. J. Wang, J. F. Donegan, J. C. Grunlan, G. Moriarty, A. Shmeliov, R. J. Nicholls, J. M. Perkins, E. M. Grieveson, K. Theuwissen, D. W. McComb, P. D. Nellist and V. Nicolosi, *Science*, 2011, **331**, 568; (d) W. Guo, C. Cheng, Y. Wu, Y. Jiang, J. Gao, D. Li and L. Jiang, *Adv. Mater.*, 2013, **25**, 6064.

10 R. T. Downs and M. Hall-Wallace, *Am. Mineral.*, 2003, 88, 247.
11 R. Spohr, *Radiat. Meas.*, 2005, **40**, 191.
12 J. Gao, W. Guo, H. Geng, X. Hou, Z. Shuai and L. Jiang, *Nano Res.*, 2011, **5**, 99.
13 I. Jung, M. Pelton, R. Piner, D. A. Dikin, S. Stankovich, S. Watcharotone, M. Hausner and R. S. Ruoff, *Nano Lett.*, 2007, **7**, 3569.
14 P. Jin, H. Mukaibo, L. P. Horne, G. W. Bishop and C. R. Martin, *J. Am. Chem. Soc.*, 2010, **132**, 2118.
15 D. Stein, M. Kruithof and C. Dekker, *Phys. Rev. Lett.*, 2004, **93**, 035901.
16 R. B. Schoch, J. Y. Han and P. Renaud, *Rev. Mod. Phys.*, 2008, **80**, 839.
17 P. Apel, *Radiat. Meas.*, 2001, **34**, 559.
18 V. Nicolosi, M. Chhowalla, M. G. Kanatzidis, M. S. Strano and J. N. Coleman, *Science*, 2013, **340**, 1226419.

Cite this: DOI: 10.1039/c0xx00000x

www.rsc.org/xxxxxx

ARTICLE TYPE

Graphical Table of Contents